New Journal of Physics
An Institute of Physics and Deutsche Physikalische Gesellschaft Journal

The influence of opacity on hydrogen excited-state population and applications to low-temperature plasmas

K Behringer[1] **and U Fantz**[2]

[1] Max-Planck-Institut für Plasmaphysik, EURATOM Association, Boltzmannstraße 2, D-85748 Garching, Germany
[2] Lehrstuhl für Experimentelle Plasmaphysik, Institut für Physik, Universität Augsburg, Universitätsstraße 1, D-86135 Augsburg, Germany
E-mail: fantz@physik.uni-augsburg.de

New Journal of Physics **2** (2000) 23.1–23.19 (http://www.njp.org/)
Received 28 April 2000; online 13 September 2000

Abstract. Atomic hydrogen lines and line ratios are being used for diagnostics of technical plasmas in hydrogen or of edge plasmas in fusion research. In the presence of hydrogen molecules, dissociative excitation also contributes to this radiation. The H Lyman lines become optically thick quite easily, which modifies the excited-state population and ionization balance. Line ratios are then a function of electron temperature and density, but also of molecular densities and opacity. To quantify these effects, collisional-radiative population calculations were carried out for the conditions of technical low-pressure plasmas using the most recent hydrogen cross sections and population escape factors. The model for computing opacity is described and results are shown as a function of optical depth. Various spatial emission profiles and spectral line profiles can be included. These results allow the analysis of hydrogen lines from low-temperature plasmas. Measurements are presented, which were carried out in microwave discharges in mixtures of hydrogen or of deuterium and helium. Atom densities and dissociation degrees were determined from absolute Balmer line intensities and from line ratios. The effects of non-Maxwellian electron energy distributions are briefly discussed. The results demonstrate the influence of dissociative excitation and opacity. Taking into account these processes, very consistent results were obtained within the experimental error limits, thus confirming the analysis methods and the rate coefficients used. Dissociation degrees of 0.1–10% were measured depending on pressure and hydrogen concentration. For standard diagnostics, a suitable method can be chosen according to the experimental conditions.

1. Introduction

Plasmas in controlled thermonuclear fusion research consist of atomic hydrogen or its isotopes. Hydrogen is also a very important constituent of many technical plasma applications (see, e.g., [1] for a discussion of hydrogen in chemical plasma processing). Consequently, atomic hydrogen line intensities and line ratios are frequently used for the determination of plasma parameters, hydrogen number densities and other quantities such as particle fluxes or ion recombination processes, both in fusion research, particularly in the plasma boundary or in divertors, and, also, in reactors for technical plasma applications. Theoretical models for hydrogen excitation and ionization have long been known, for example Johnson and Hinnov [2] or Drawin and Emard [3]. The rate coefficients in these calculations were mostly based on Coulomb–Born calculations. Very recently, substantially improved R-matrix cross sections for atomic hydrogen became available [4] and were implemented in the ADAS (Atomic Data Analysis System) atomic data and program package [5]. They will be applied to plasma spectroscopy here for the first time. In technical plasmas, where a substantial fraction of hydrogen molecules is present, the contribution of H_2 dissociative excitation or other molecular processes to the Balmer or Lyman line radiation can be very important, modifying hydrogen excited state population and Balmer line intensity ratios. Cross sections for this process have been studied, for example by Möhlmann *et al* [6], and this excitation path is included in Sawada and Fujimoto's collisional-radiative model for atomic and molecular hydrogen [7]. In all models, it was acknowledged that the Lyman lines may become optically thick in the considered plasmas and this opacity was included in more or less sophisticated ways. The optical thickness of the resonance lines plays a very important role in many low-density, low-temperature discharges for plasma technology. The radiative transfer in hydrogen resonance lines has also become an important issue in present-day divertor plasmas, as, for example, realized in ASDEX Upgrade [8], due to strong net volume recombination resulting in high neutral densities. This opacity affects the emitted radiance of spectral lines, but also changes the population of excited states, line intensity ratios and the effective collisional-radiative ionization and recombination rate coefficients. In order to deal with the consequences of radiative transfer, the escape factor method has been widely used in astrophysics and plasma physics (see, for example, Irons [9] for an overview) and the present analysis is based on the same approach.

In this paper, a detailed investigation of hydrogen line excitation in low-temperature plasmas is presented. Special emphasis is being placed on the influence of dissociative excitation and on the consequences of opacity. For the latter purpose, hydrogen escape factors were calculated, on the basis of some simplifying assumptions, by a computer code, which has become part of the ADAS atomic physics package [5]. The change in excited state population and ionization balance due to the reabsorption of radiation are presented. Experiments were carried out in microwave plasmas, demonstrating the importance of these effects and identifying the spectral lines which are least affected and therefore most suitable for diagnostics, for example, of plasmas for technical processing.

2. Excitation models and rate coefficients

In low-density plasmas, the corona model for excitation is often adopted, i.e. the balance between electron impact excitation and spontaneous decay. Furthermore, all particles are assumed to be

in the ground state with density n_1. In the simplest case, this leads to

$$n_1 n_\mathrm{e} X^a_{1,m}(T_\mathrm{e}) = n^a_m \sum_{k<m} A_{m,k} \tag{1}$$

with the electron density n_e, the rate coefficient for electron impact excitation $X_{1,m}$ and the Einstein coefficients A. The rate coefficients are obtained by integration of the cross sections over the electron energy distribution function (EEDF) and, in the case of a Maxwellian, only depend on the electron temperature T_e. In our case, the hydrogen excited state density n^a_m in state m originates from excitation within the hydrogen atom with the ground-state density n_1. The emitted photon number in transition $m \to j$ per unit volume and time, $N^a_{\mathrm{Ph},m,j}$, is then given by

$$N^a_{\mathrm{Ph},m,j} = n_1 n_\mathrm{e} X^a_{1,m} \frac{A_{m,j}}{\sum A_{m,k}} = n_1 n_\mathrm{e} X^a_{1,m} B_{m,j} = n_1 n_\mathrm{e} X^a_{\mathrm{em},m,j} \tag{2}$$

where B is the branching ratio and X_em the emission rate coefficient. The line emission coefficient ε_L is obtained by multiplication with $h\nu/4\pi$. In low-temperature plasmas with H_2 molecules, dissociative excitation processes into level m must also be taken into account, which are often a very important contribution. They can be accommodated within the corona model by the additional term $n_\mathrm{M} n_\mathrm{e} X^\mathrm{M}_m(T_\mathrm{e})$ on the left-hand side of equation (1) with the molecular density n_M and the molecular excitation rate coefficient X^M_m. This gives the total number $n_m = n^a_m + n^\mathrm{M}_m$ in state m and the corresponding photon emission coefficient according to equation (2). Dissociative recombination of H_2^+ also leads to the formation of excited hydrogen atoms and could be included by the formalism for H_2 described below. However, in the considered plasmas, the H_2^+ densities are very small and can be neglected. A Maxwellian electron energy distribution is adopted in the following discussion, but its existence must be verified in each case, a problem which will be addressed in the experimental section. The pertinent excitation cross sections could also be averaged over other EEDFs.

The basic corona model must be complemented by cascading, ionization, redistribution among excited states, quenching and other processes. In cases other than hydrogen, metastable levels must be included. The results of such collisional-radiative models are metastable-resolved effective rate coefficients $X_\mathrm{eff}(T_\mathrm{e}, n_\mathrm{e}, \ldots)$, which can, for example, be obtained by the ADAS atomic physics package. The ADAS program calculates the dependence of the excited state population on the ground and metastable levels, on ion densities via recombination and possibly on charge exchange processes. The resulting coefficients must be multiplied by the pertinent particle densities, for example by $n_1 n_\mathrm{e}$ for ground-state excitation. ADAS also gives the effective ionization rate coefficient S_1 and the recombination rate coefficient α_1, both referring to the ground state. ADAS has been used for the present analysis of hydrogen line radiation. Effective ADAS emission rate coefficients for three Balmer lines, based on recent high-quality R-matrix cross sections [4], are shown in figure 1 as a function of T_e and for $n_\mathrm{e} = 10^{17}\ \mathrm{m}^{-3}$. In comparison with these data, the often used, older results of Johnson and Hinnov [2] are considerably higher, for example for $T_\mathrm{e} = 3$ eV and H_α by a factor of 1.5, for H_β and H_γ by a factor of 2. ADAS can also deal with the dissociative excitation of hydrogen or deuterium molecules as an additional excitation path, thus including cascading, ionization and redistribution for the molecular part. The dependences of these Balmer lines on the molecule densities and temperature are also plotted in figure 1 for the same n_e. The rate coefficients into $n = 3$, 4 and 5 were based on the experimental cross sections of Möhlmann *et al* [6], the hydrogen data for $n = 2$ were taken from Tawara *et al* [10] and scaled to deuterium [11]. It may be worth noting that the contribution of dissociative excitation is substantially smaller for deuterium than for hydrogen.

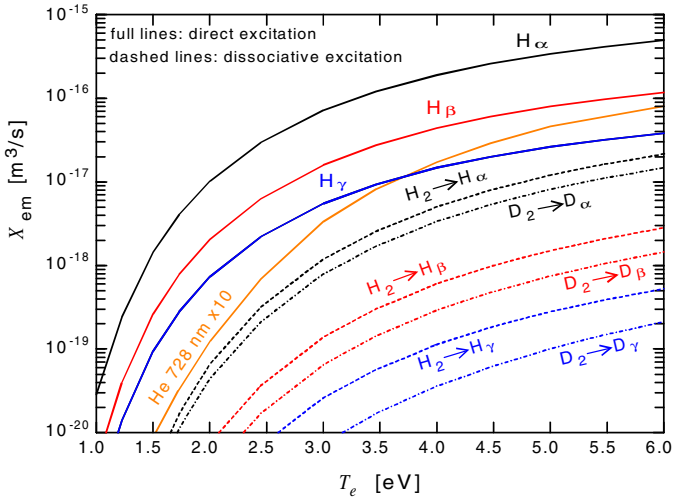

Figure 1. Emission rate coefficients for three Balmer lines. The full curves denote the effective atomic excitation calculated by ADAS, the broken curves are the dissociative excitation coefficients for the H_2 and D_2 molecules. The optically thin He emission coefficient for the transition $3s\,^1S$–$2p\,^1P$ at 728.1 nm is also shown (marked full curve). All data refer to $n_e = 10^{17}\ m^{-3}$.

For both isotopes, the molecular excitation rate coefficients decrease faster with higher quantum number n than the atomic ones, because of the increasing threshold energy of those processes. Therefore, the influence of dissociative excitation on the Balmer lines also decreases with n. For direct excitation, there is no difference between hydrogen and deuterium. In the optically-thin case and for these low electron densities, the effective rate coefficients are only about 10% different from the simple direct ones.

If the lower state of a particular atomic transition is significantly populated and the plasma size is large enough, radiation may not be able to escape, but may at least be partly reabsorbed in the plasma. In this case, the spectral radiance must be calculated from the radiative transport equation using the spectral emission coefficient $\varepsilon_\lambda(\lambda)$ and the absorption coefficient $\kappa(\lambda)$ as a function of wavelength. The reduction of the emitted radiation can be described by introducing escape factors $\Theta_R \leq 1$ and reducing the optically-thin transition probabilities. Another consequence is an increase in the excited-state population, which can also influence other optically-thin spectral lines with the same upper level or by redistribution. This effect will be described by population escape factors Θ_P or just Θ. These population escape factors can be defined by a further amendment to the steady-state collisional-radiative balance of populating and depopulating reactions for level m:

$$\sum_{k\neq m} n_k n_e X^a_{k,m} + \sum_{k<m} \int_{\text{line}} \int_\Omega \frac{\kappa_{k,m}(\lambda)}{h\nu} L_\lambda(\lambda,\Omega)\,\mathrm{d}\Omega\,\mathrm{d}\lambda + \cdots = n^a_m \sum_{k<m} A_{m,k} + n^a_m n_e \Big(\sum_{k\neq m} X_{m,k} + \cdots \Big). \tag{3}$$

In equation (3), the first sum denotes all the populating electron collisions from other levels, k in our case, particularly from the ground state. The second term stands for the absorption processes from all lower levels due to the spectral line absorption coefficients $\kappa_{k,m}(\lambda)$ and the

spectral radiance L_λ at the considered position in the plasma. This radiance is in turn caused by transitions from level m to lower states k and must be calculated from the radiation transport equation. Absorption is proportional to the numbers in lower states and is particularly important from the ground state. Strictly speaking, $\kappa_{k,m}(\lambda)$ is the net absorption coefficient, i.e. the absorption minus stimulated emission. However, the latter is of very little importance for the conditions discussed here and has been neglected. The product κL_λ must be integrated over the spectral line profiles and all directions, characterized by the solid angle Ω. It involves both absorption and emission line profiles, which are usually assumed to be equal. Other populating processes, such as cascading and recombination must be added. The right-hand side comprises all the depopulating reactions, in low-density plasmas this is mainly spontaneous decay to lower levels k as discussed above. Electron collisions of the second kind and redistribution with coefficients $X_{m,k}$ are given explicitly. They must be complemented by ionization and other depopulating collisions. Subtracting the absorption from the spontaneous emission, one obtains

$$\begin{aligned}\sum_{k\neq m} n_k n_\mathrm{e} X^a_{k,m} + \cdots \\ &= n^a_m \sum_{k<m} A_{m,k}\left(1 - \frac{1}{n^a_m A_{m,k} h\nu}\int_\mathrm{line}\int_\Omega \kappa_{k,m}(\lambda) L_\lambda(\lambda,\Omega)\,\mathrm{d}\Omega\,\mathrm{d}\lambda\right) + n^a_m n_\mathrm{e}(\cdots) \\ &= n^a_m \sum_{k<m} A_{m,k}\Theta_{m,k} + n^a_m n_\mathrm{e}(\cdots) \qquad (4)\end{aligned}$$

which is the definition of the population escape factors. The optically-thin transition probabilities are reduced by the ratio of the absorbed-to-emitted radiation power. The excited state density n^a_m in Θ cancels, since it also appears in L_λ. The consequences of absorption can be defined as correction factors k to the optically-thin effective emission rate coefficients.

Adding dissociative excitation of molecules, the sum of all states n_m is given by

$$n_m = \frac{\sum_{k\neq m} n_k n_\mathrm{e} X^a_{k,m} + n_\mathrm{M} n_\mathrm{e} X^\mathrm{M}_m + \cdots}{\sum_{k<m} A_{m,k}\Theta^*_{m,k} + \cdots} \qquad (5)$$

with

$$\Theta^*_{m,k} = 1 - \frac{1}{n_m A_{m,k} h\nu}\int_\mathrm{line}\int_\Omega \kappa_{k,m}(\lambda) L_\lambda(\lambda,\Omega)\,\mathrm{d}\Omega\,\mathrm{d}\lambda. \qquad (6)$$

The ADAS collisional-radiative code solves (5) for all m including atomic and molecular excitation and yields the dependences on both densities. It also provides corrections for predefined escape factors Θ^* of the resonance lines.

For calculating the spectral radiance in Θ^*, the contribution of the molecules must be included, i.e. the total n_m must be used. However, the spectral line profiles of dissociative excitation processes could be broader than those of the usual hydrogen lines, since the particles gain kinetic energy from this reaction. A study of escape factors for spectral emission profiles wider than the relevant absorption profiles will be shown below. If dissociative excitation is important, one could assume the same spectral line profiles for atoms and molecules and proceed as for atoms alone. Another possibility consists of neglecting the reabsorption of light from dissociative excitation altogether, due to its wider spectral profiles. In this case, the molecular excitation must be added separately using the optically-thin emission rate coefficients from a second collisional-radiative calculation.

In the present experiments, atomic H/D lines were investigated in mixtures of hydrogen and deuterium with helium. Helium increases the electron temperature and dissociation

degree as explained below. It was therefore only natural to use helium emission lines for the measurements of the electron temperature. However, the above arguments for the collisional-radiative calculations and the opacity of the resonance lines equally apply to He and, here again, several models exist, for example by Fujimoto [12]. Fujimoto's collisional-radiative model was originally based on Born excitation cross sections. However, over the last few years, electron excitation cross sections of helium were also revised and re-calculated using the R-matrix method [13]. The new cross sections should be more accurate, particularly near the threshold energy, which is of high importance here. These data have been included in ADAS and also in Fujimoto's collisional-radiative code [14]. Either one could have been used for the present diagnostics, but the opacity of the resonance lines and the diffusion of the metastable states had to be implemented. A detailed discussion of many transitions, as well as experimental results will be published elsewhere. For the present study, only one line was employed, which is that least sensitive to the optical thickness and metastable diffusion, i.e. the transition $3\mathrm{s}\,{}^1\mathrm{S}$–$2\mathrm{p}\,{}^1\mathrm{P}$ at 728.1 nm. The calculation was performed by ADAS, taking into account diffusion by artificially introducing transition probabilities from the metastable states to the ground state. The new atomic data result in an increase of a factor of four in the pertinent rate coefficient over Fujimoto's original model. As an example, the optically-thin emission rate coefficient is also shown in figure 1 as a function of T_e. It increases roughly by a factor of two due to opacity in the present helium plasmas.

3. Population escape factor calculations

Calculations of the population escape factors and the approximations used have been described in detail in a previous report [15]. Therefore, only a short overview shall be given. If the plasma extends over coordinate ℓ from zero to b, the spectral radiance at b is

$$L_\lambda(b) = \int_0^b \varepsilon_\lambda(\ell) \exp\left[-\int_\ell^b \kappa(\ell')\,\mathrm{d}\ell'\right]\mathrm{d}\ell + L_\lambda(0)\exp\left[-\int_0^b \kappa(\ell)\,\mathrm{d}\ell\right]. \qquad (7)$$

Normally, $L_\lambda(0) = 0$. In the following, the assumption was made that κ is independent of ℓ, i.e. that the neutral density is constant in space, which is quite true for low-density plasmas and to a first approximation of the conditions in low-temperature divertors. The spectral emission coefficients can be derived from the line emission coefficients ε_L and the spectral line profiles $P_\lambda(\lambda)$, which must be calculated on the basis of the relevant line broadening mechanisms in the plasmas. Here, mainly Doppler broadening is important.

As a further simplification, spatially constant line profiles $P_\lambda(\lambda)$ were assumed for both emission and absorption. Again, this limitation should not be too severe, if P_λ is a Doppler profile determined by the thermal motion of the neutral particles, either due to the gas temperature, or on the basis of their Franck–Condon energy or charge exchange temperature. In the latter case, the mean free path of these particles is often long compared to the plasma dimensions and gradients should not develop. For higher electron densities, the linear Stark effect must be superimposed, particularly in the line wings, which was done for analysis of ASDEX Upgrade divertor radiation including Zeeman splitting [15]. In technical plasmas with low gas temperatures, the fine-structure splitting of hydrogen levels represents a lower limit for the line widths, which may be of the order of the Doppler effect. Various line profiles and convolutions can be used in the calculations, however, for the present analysis, only Doppler profiles are of interest. The code can also take into account different absorption and emission line profiles.

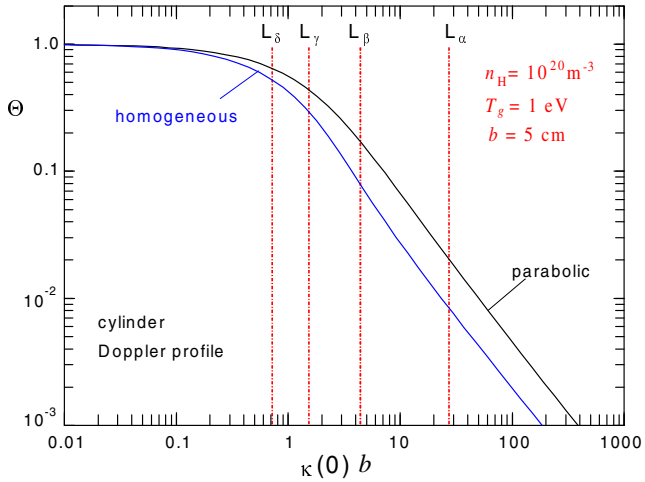

Figure 2. Examples of the population escape factors for the axis of a cylinder of radius b. Only Doppler broadening is included. The positions of hydrogen Lyman lines are indicated for the annotated plasma parameters.

The absorption power in the plasma per unit volume and time must be evaluated from the spectral radiance $L_\lambda(\lambda)$ at the relevant plasma location times the effective absorption coefficient $\kappa(\lambda)$, integrated over the wavelength and the solid angle Ω. The emitted power is given by $4\pi\varepsilon_\mathrm{L}$. The present calculations were restricted to the centre of a plasma sphere, of a plasma disk, or to the axis of a plasma cylinder [15]. A point or line symmetry was adopted for the plasma parameters. If the population is evaluated for position $\ell = b$ (radius or thickness) in the centre of the plasma and the plasma edge is at $\ell = 0$, the escape factor becomes

$$\Theta = 1 - \frac{\int_\Omega \int_\mathrm{line} \kappa(\lambda) \int_0^b \varepsilon_\lambda(\ell, \lambda) \exp[(\ell - b)\kappa(\lambda)] \, \mathrm{d}\ell(\Omega) \, \mathrm{d}\lambda \, \mathrm{d}\Omega}{4\pi\varepsilon_\mathrm{L}(b)}. \tag{8}$$

For a given line profile, Θ only depends on the product of the absorption coefficient in the line centre, $\kappa(0)$ and the relevant length b.

The spectral radiance in this relation for Θ was worked out by a polynomial fit to the spatial profile of the emission coefficient and by integration by parts. Three spatial intensity profiles were investigated, namely, constant emission over ℓ, a linear increase from the edge to the plasma centre and a parabolic shape with the maximum in the centre of the plasma. The population escape factor for spatially constant and isotropic radiation becomes, for example,

$$\Theta = 1 - \frac{\int_\mathrm{line} \varepsilon_\lambda [1 - \exp(-\kappa b)] \, \mathrm{d}\lambda}{\varepsilon_\mathrm{L}} = \int_\mathrm{line} P_\lambda \exp(-\kappa b) \, \mathrm{d}\lambda. \tag{9}$$

After integration over the spectral line profiles, the line escape factors are readily calculated. Examples for the axis of a plasma cylinder and Doppler profiles are shown in figure 2. The results apply to constant spatial emission and a parabolic spatial profile. The spectral emission and absorption profiles are assumed to be equal. Also indicated are the optical thicknesses of the hydrogen Lyman lines for the following conditions: neutral hydrogen density $n_\mathrm{H} = 10^{20}$ m^{-3}, gas temperature $T_\mathrm{g} = 1$ eV, atomic mass number $\mu = 1$ and radius of the plasma cylinder $b = 5$ cm. All figures in the following section refer to these conditions, except for variation of

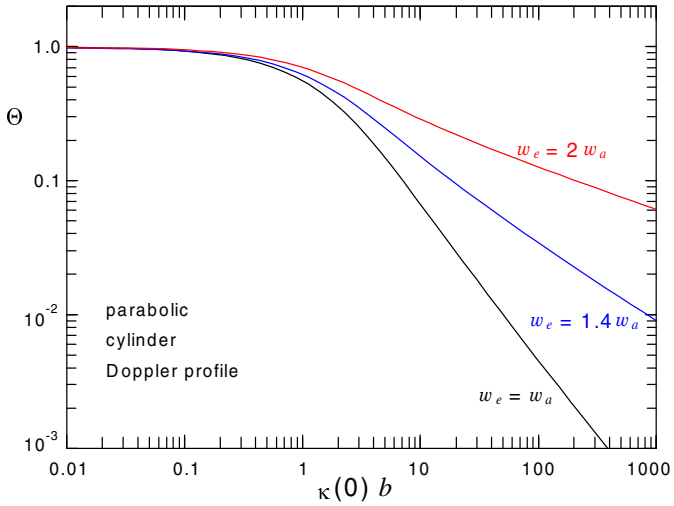

Figure 3. Escape factors for Doppler emission line widths w_{e} and absorption line widths w_{a} for estimating the effect of the wider emission profiles, as expected, for dissociative excitation.

the neutral density. The value of $\kappa(0)$ is proportional to n_{H}, oscillator strength f, λ and $\sqrt{\mu/T_{\mathrm{g}}}$:

$$\kappa(0) = n_{\mathrm{H}} \frac{\lambda}{c} \frac{fe^2}{4\varepsilon_0 m_{\mathrm{e}}} \sqrt{\frac{\mu m_p}{2\pi k T_{\mathrm{g}}}}. \tag{10}$$

Because of the importance of the dissociative excitation, the calculations were carried out with emission profiles of larger widths than the absorption profiles. Two examples are shown in figure 3 for absorption Doppler widths w_{a} and emission Doppler widths w_{e}, where $w_{\mathrm{e}} = 1.4 w_{\mathrm{a}}$ and $w_{\mathrm{e}} = 2 w_{\mathrm{a}}$. As could be expected, much less of the radiation power can be re-absorbed if $w_{\mathrm{e}} > w_{\mathrm{a}}$, and the corresponding escape factors are much higher in those cases.

The described population escape factors were used to modify the transition probabilities of the atomic input data sets to the ADAS population programs. Subsequently, collisional-radiative level calculations were carried out resulting in population dependences on atomic ground-state numbers, molecular densities and recombining ion densities.

4. Theoretical results for optically-thick excited-state populations

Figure 4 shows the consequences of optical thickness on the population of excited hydrogen levels with $n = 2$ and $n = 3$, as calculated by the ADAS program. For zero absorption and low electron densities, these states are in corona excitation balance, i.e. the ratio $n_m/(n_1 n_{\mathrm{e}})$ is independent of the electron density. At high n_{e}, the populations approach Boltzmann equilibrium with $n_m/(n_1 n_{\mathrm{e}})$ proportional to $1/n_{\mathrm{e}}$, provided that the ionization losses are compensated by recombination. If the ion densities are much smaller than their equilibrium values, the populations also become independent of n_{e}, since collisions are much more frequent than radiative transitions. However, their absolute values are lower than the Boltzmann equilibrium due to the imbalanced ionization losses. As soon as the absorption of the Lyman lines is important, the $n = 2$ population strongly increases due to the optical thickness of L_α; L_β is always much less affected. This higher population is more and more redistributed to $n = 3$ and other levels at higher electron

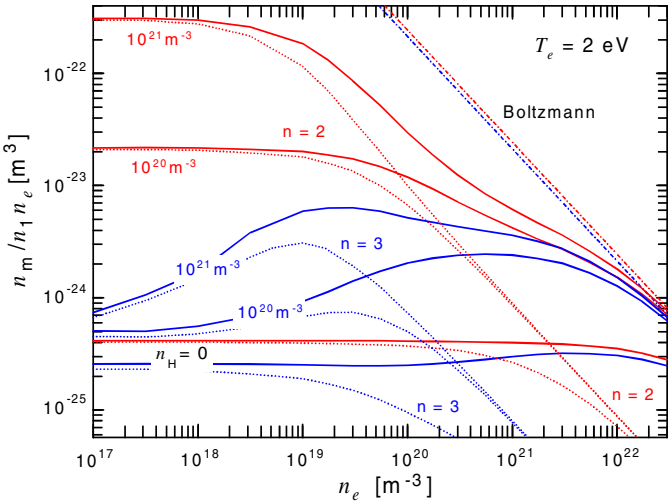

Figure 4. ADAS calculations for the population of $n = 2$ and $n = 3$ excited hydrogen levels as a function of the electron density for the optically-thin case ($n_{\mathrm{H}} = 0$) and two values of opacity. The broken curves are with small ionization degree, for the full curves the ionization balance and recombination are set to the atomic physics prediction.

densities. With balanced ionization, the Boltzmann equilibrium is reached at lower n_{e}, i.e. at about 3×10^{22} m^{-3} for the cases above. The neutral densities in figure 4 correspond to the typical range for technical plasmas or divertors. Two conclusions may be interesting to note, namely, at low electron densities in technical plasmas, $n = 2$ will always be orders of magnitude below the Boltzmann value and therefore, H_α will always be optically thin. Secondly, in arc plasmas at atmospheric pressure, as investigated widely some 30 years ago, the assumption of a Boltzmann distribution is justified, at least for $n_{\mathrm{e}} > 10^{23}$ m^{-3}. Apparently, thermal equilibrium can only be established for all levels simultaneously and the Saha ionization balance is also required.

As can be concluded from figure 4, the emission coefficient of H_α (and of other Balmer lines) will not only depend on the electron density and temperature, but also on the neutral atom densities. Calculations of the latter influence are shown in figure 5 for the Balmer lines H_α, H_β and H_γ with $T_{\mathrm{e}} = 2$ eV and $n_{\mathrm{e}} = 10^{17}$ m^{-3}, i.e. roughly for the conditions found in technical low-pressure discharges. They are valid for a 1 eV Doppler profile and must be scaled to the actual T_{g}. Shown are the factors k to be applied to results for optically-thin calculations, in order to account for the opacity of the resonance lines. They depend on the electron density and, to a lesser extent, on the electron temperature. Including dissociative excitation in ADAS, correction factors can also be obtained for the molecular part. For H_α, these are quite similar to those in figure 5. The factors for H_β and H_γ are somewhat higher at higher neutral densities. For simplicity, the shown correction factors will be applied both to the atomic and the molecular contributions in the following analysis.

From figure 5, it can be concluded that line intensity ratios between the Balmer lines will also be modified by the optical thickness of the resonance transitions, since H_α is affected earlier than the other lines. Two sensitive ratios, i.e. $\mathrm{H}_\alpha/\mathrm{H}_\beta$ and $\mathrm{H}_\alpha/\mathrm{H}_\gamma$, are shown in figure 6 for $T_{\mathrm{e}} = 2$ eV and $T_{\mathrm{e}} = 5$ eV as functions of the neutral hydrogen density or optical thickness. The horizontal lines at the left-hand margin are the optically-thin ratios; on the right-hand side

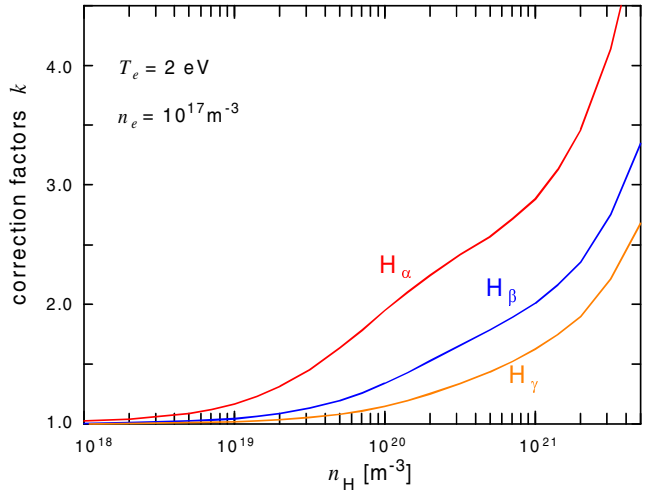

Figure 5. Correction factors for H_α, H_β and H_γ to account for optical thickness of the Lyman resonance lines. The calculations are valid for a Doppler profile with $T_g = 1$ eV and must be scaled to the actual conditions. They are electron density and temperature dependent.

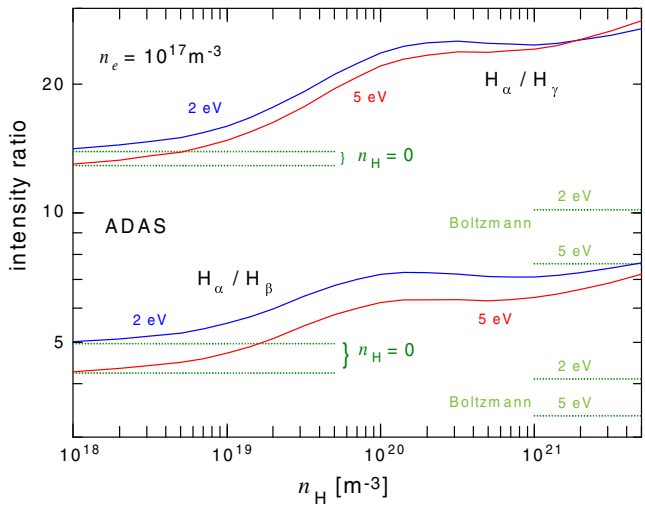

Figure 6. The Balmer line ratios for two electron temperatures as functions of the neutral hydrogen density, i.e. the opacity of the Lyman lines. These ratios depend on n_e, T_e, the neutral hydrogen density and on the contributions from molecular dissociative excitation, as shown below.

the ratios in Boltzmann equilibrium are given for comparison. In low-temperature, low-density plasmas, the Balmer line ratios are a function of the electron density, electron temperature, neutral hydrogen density and the contribution from molecular dissociative excitation. They could serve as diagnostic tools for one of these parameters, if the others are well known and if the theoretical description is precise enough.

The ionization balance is also modified by the opacity of the resonance lines. As an example, figure 7 shows the ADAS calculations of the effective ionization and recombination

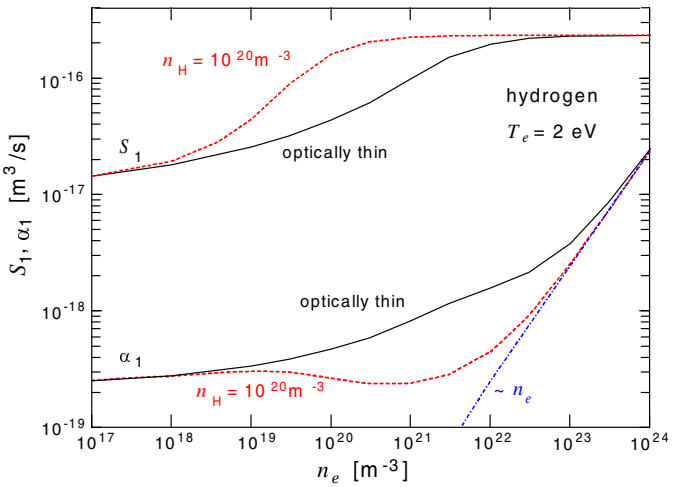

Figure 7. Hydrogen ionization and recombination coefficients for 2 eV as a function of the electron density. An example of optical thickness is shown, increasing S_1 via stepwise ionization and reducing α_1, since both coefficients are defined with respect to the ground state.

rate coefficients as functions of the electron density and for a temperature of 2 eV. The ionization rate coefficients increase with electron density and with optical thickness due to stepwise ionization until a Boltzmann distribution is established amongst the excited levels. Then they are independent of n_e, except for the lowering of the ionization potential, which is not considered here. At low electron densities, the main recombination process is radiative recombination and possible molecular reactions. At higher n_e, three-body recombination first into excited states and then also into the ground state becomes more and more important until α_1 is proportional to electron density, which corresponds to Saha equilibrium. In the transition region, α_1 is modified by the optical thickness of the resonance lines, since the coefficient is defined as recombination into the ground state and recombination into excited levels must therefore be followed by spontaneous decay. The latter is partly compensated by absorption processes in the case of opacity and α_1 is reduced.

In the absence of diffusion, the ratio of ion and neutral ground-state densities n_i/n_1 is given by S_1/α_1. In order to obtain the ratio of ions to all neutrals, the excited states must be added, i.e. the partition function taken into account. At low densities, this correction is small due to the substantial underpopulation of excited levels. From figure 7 it can be concluded that the ionization balance in the absence of diffusion would be roughly $n_i/n_H = 100$ for $T_e = 2$ eV. In real low-pressure plasmas for technical applications at this electron temperature n_i/n_H is about 10^{-4}. Stepwise ionization plays a minor role.

5. Experiment

For an experimental cross-check of the described hydrogen calculations including dissociative excitation and opacity, low-pressure plasmas in hydrogen–helium mixtures were investigated. These were ECR (electron cyclotron resonance heated) plasmas at a frequency of 2.45 GHz with a maximum of 100 W input power. The resonant magnetic field strength of 0.0875 T was

produced by two rows of permanent magnets of 1 T each at the surface. In the resonance zone, approximately 1 cm above the plate, these plasmas are preferentially heated and diffuse into the vessel volume. A detailed description of the experimental set-up is given in [16]. The pressure range was 2–20 Pa, measured with a Baratron pressure gauge. The plasma volume depends on the gas mixture and pressure, and is typically about $500\ \mathrm{cm}^3$.

For the analysis of the plasma radiation, a 1 m SPEX spectrometer was used with a 2D-CCD camera as a detector. The spectral resolution was about 55 pm and the optical system was absolutely calibrated by means of a tungsten ribbon lamb (Osram WI17/G) in the wavelength range 350–900 nm. The lines of sight were aligned parallel to the two permanent magnets in the centre, with the spatial resolution perpendicular to the base plate. The plasmas were assumed to be homogeneous along the lines of sight, because they are in the diffusion dominated region. The plasma length was approximately 10 cm, the length of the magnets was 8 cm. The accuracy of the measured line emission coefficients is expected to be better than $\pm 25\%$ due to uncertainties of calibration, spectral line integration and plasma length. The relative errors in line ratios should be less than 10% and are limited by the plasma stability.

The electron temperatures in low-pressure plasmas are determined by a balance of ionization, given by the ionization rate coefficients, the neutral density and the ambipolar diffusion losses. Therefore, substituting some of the hydrogen gas by helium leads to higher temperatures, which must compensate for the smaller He ionization rate coefficient. Lower pressures also increase T_e, and diffusion. Deuterium has higher mass than hydrogen and therefore, the diffusion coefficients are smaller. Consequently, somewhat lower electron temperatures are expected and found in D_2 than in H_2. Higher T_e values result in higher degrees of dissociation of hydrogen molecules, which is the reason for using mixtures with helium here.

6. Diagnostics

The plasma parameters were determined by various diagnostic methods. The electron density was about $9 \times 10^{16}\ \mathrm{m}^{-3}$ in all plasmas, as measured by microwave interferometry, using the same line of sight as the optical system. The ionization degree was thus of the order of 10^{-4}, the precise value depending on pressure. A gas temperature of 450 K, again independent of the detailed conditions, was derived from the rotational temperature of the $v = 0$ to $v = 2$ vibrational transition in the second positive system of N_2 at 380 nm.

Assuming a Maxwellian EEDF, the T_e values were obtained from the radiation of the He 728.1 nm line, using the effective emission rate coefficients discussed in section 2. Quenching by hydrogen molecules was considered, but is small. Using the rate coefficient from [17], a maximum influence of 10% must be expected for the present conditions with very little influence on T_e. To check the existence of a Maxwellian distribution, a spectroscopic method was employed, which is described in [18] and is based on comparing the Ar and He lines with very different threshold energies. In the energy range of these excitation cross sections, the EEDF can be fitted by an analytic formula [18] and the cross sections can be integrated over this approximate function. These investigations were carried out separately from the hydrogen measurements, since the metastable argon states appeared to influence the hydrogen line radiation. The argon concentration was less than 1%. It turned out that, in the cases of low pressures and small amounts of hydrogen in helium, the EEDF was quite Maxwellian, while increasingly stronger deviations were observed for higher pressures and hydrogen concentrations.

Electron temperatures or EEDFs were required for calculating the contribution of dissociative excitation to the hydrogen line radiation and for deriving the hydrogen atomic densities. For interpreting the line ratios, they are of lesser importance; in particular, if molecular contributions are either very small or very high. Since the purpose of the present analysis was mainly a demonstration of methods, detailed comparisons were restricted to the simpler cases with low molecular content and/or low pressures. Reasonable results were still obtained for the other plasmas.

Electron temperatures derived from the He 728 nm line were 3.2–2.2 eV for 10% H_2 in He and pressures between 4 and 18 Pa. For 90% H_2 in He, T_e was found to be 2.2–1.7 eV in the same pressure range. In the latter case, there is an noticeable difference between hydrogen and deuterium, which had about 5% lower temperatures.

7. Results for the degrees of hydrogen dissociation

Hydrogen atom densities and dissociation degrees were derived from the absolute intensities of three hydrogen Balmer lines. Due to the high fraction of molecules, direct atom excitation and dissociative excitation must both be taken into account in the interpretation. The hydrogen atom density n_H is then related to the measured photon emission coefficient by

$$n_H = \frac{\dot{N}_{Ph} - n_M n_e X^M_{em}(T_e)}{n_e X^a_{em}(T_e)} \tag{11}$$

with the effective emission coefficients X_{em}. The molecular density was derived from Dalton's law using the molecule partial pressure and the gas temperature. The molecular pressure was obtained from the known mixture, subtracting electron and ion pressures as well as the atom pressure—all small corrections—by iteration. Knowledge of T_e is relatively important for evaluating equation (11). Contributions to the Balmer lines from dissociative recombination or mutual H^-/H^+ recombination are negligible (below 5%) in the considered plasmas. Quenching processes by hydrogen molecules also influence the upper states of the Balmer lines only very little. Estimates on the basis of [19] show that the maximum correction is of the order of 5%, which has been taken into account in the results. Depending on the neutral hydrogen densities in these plasmas, both rate coefficients must be corrected for the optical thickness of the Lyman lines.

Figures 8 and 9 show measured H densities from H_α, H_β and H_γ (D_α, D_β and D_γ) for 10% H_2 (D_2) in helium with and without correction of the optical thickness of the Lyman lines. Under the assumption of optically-thin plasmas, the Balmer lines result in different atomic densities, particularly from H_α as compared to the other two. The discrepancy is somewhat larger for deuterium than for hydrogen (smaller Doppler profiles, higher reabsorption). Taking into account the influence of the optical thickness leads to consistent results in both gases. The error bars shown are estimates for the line emission coefficients, they do not take into account any uncertainties in the rate coefficients.

The parameters for the correction of the optical thickness were as follows: cylinder geometry with $b = 5$ cm, Doppler profile with 'T_g' $= 700$ K (line width due to thermal motion and fine-structure), parabolic spatial profile for emission and atomic mass $\mu = 1$ for H, $\mu = 2$ for D. In a first step the H_γ line was used for calculating the n_H density. This line is least influenced by opacity. Using this density, a correction factor for the excitation rates was determined from figure 5, scaled to the lower gas temperature. Subsequently, the correction was applied to the

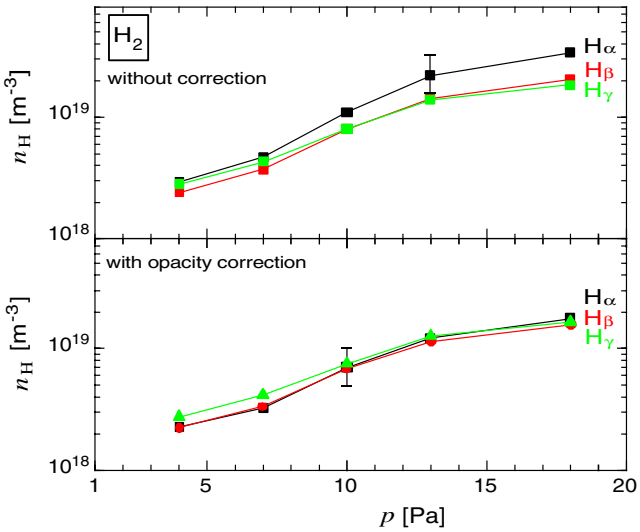

Figure 8. Atomic hydrogen densities derived from the radiation of H_α, H_β and H_γ lines in mixtures of 10% H_2 in He at various pressures.

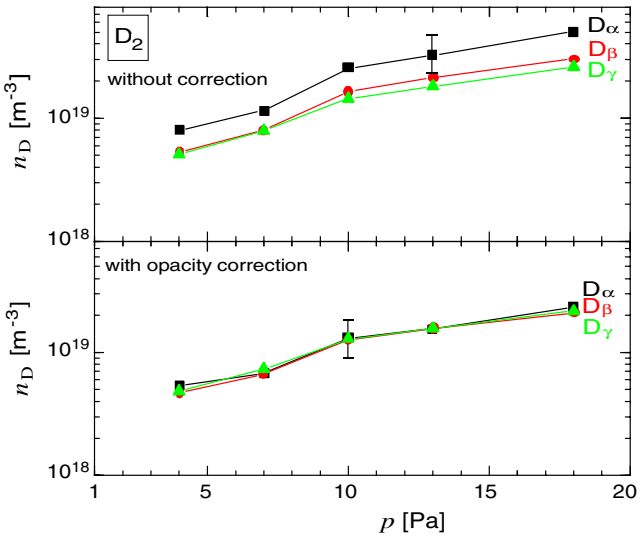

Figure 9. Atomic deuterium densities derived from the radiation of D_α, D_β and D_γ lines in mixtures of 10% D_2 in He at various pressures.

radiation of all lines. In plasmas with 10% H_2, dissociative excitation contributes less than 20% to the measured radiation and less than 8% in D_2. Therefore, the correction to the molecular part is relatively uncritical. As a consequence of the described procedure, the densities from all three Balmer lines agree well within the error bars for both hydrogen and deuterium. In the cases shown, one could just have used H_γ or D_γ, which contain the smallest molecular contribution and are least affected by opacity. However, they are the weakest lines and, depending on the ionization balance, they are most susceptible to recombination and are very electron density dependent.

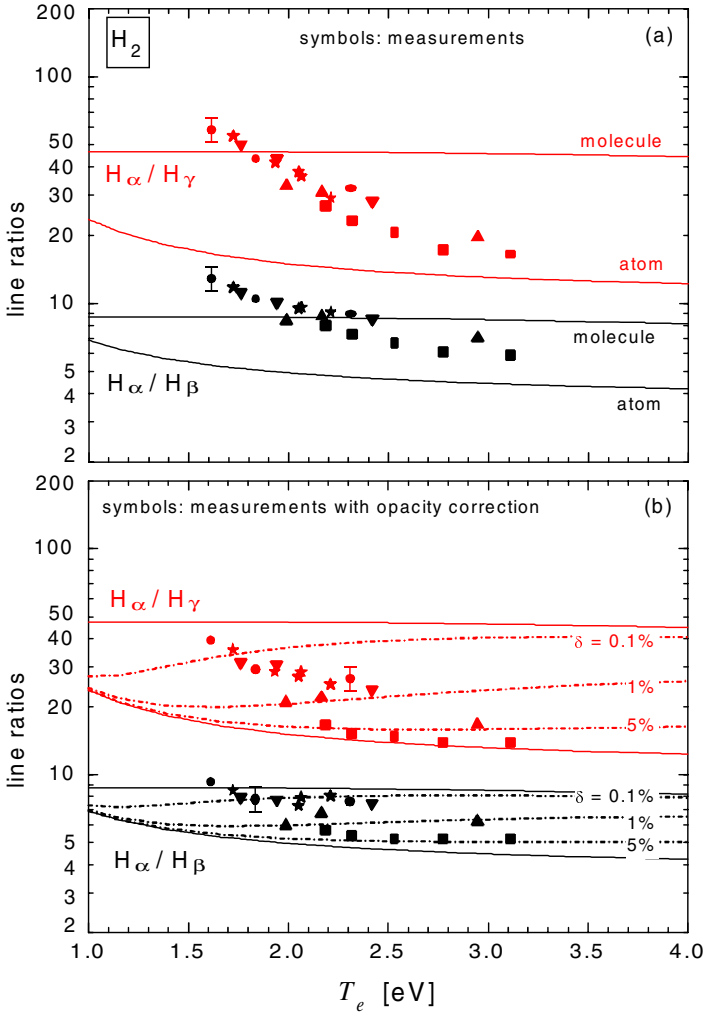

Figure 10. Balmer line ratios of H_2/He mixtures at various pressures with and without correction of the optical thickness for various degrees of dissociation. The symbols denote the mixtures: (square) 10%, (triangle up) 20%, (triangle down) 50%, (circle) 80% and (star) 90% hydrogen molecules in helium.

The dissociation degree in these mixtures, which is defined as

$$\delta = \frac{n_{\mathrm{H}}}{(n_{\mathrm{H}}/2) + n_{\mathrm{H_2}}} \tag{12}$$

was 4–6% for hydrogen in the pressure range of 4–18 Pa and slightly higher (5.5–7.5%) for deuterium due to a higher dissociation cross sections for deuterium than for hydrogen [20, 21]. Theoretical calculations give a factor 1.18 for excitation from the $v = 0$ and 1.38 from the $v = 5$ level of the ground state, which apparently over-compensates the lower electron temperature.

In helium plasmas with higher hydrogen admixtures, molecules contribute more than 50% to the Balmer radiation and, therefore, the above method is no longer suitable for n_{H} diagnostics (difference of two similar numbers with error bars). In such cases, another technique, i.e. the line ratios, may serve as a diagnostic tool for the dissociation degree, as already proposed by Schulz-von der Gathen and Döbele [22]. Here again, the influence of the optical thickness is

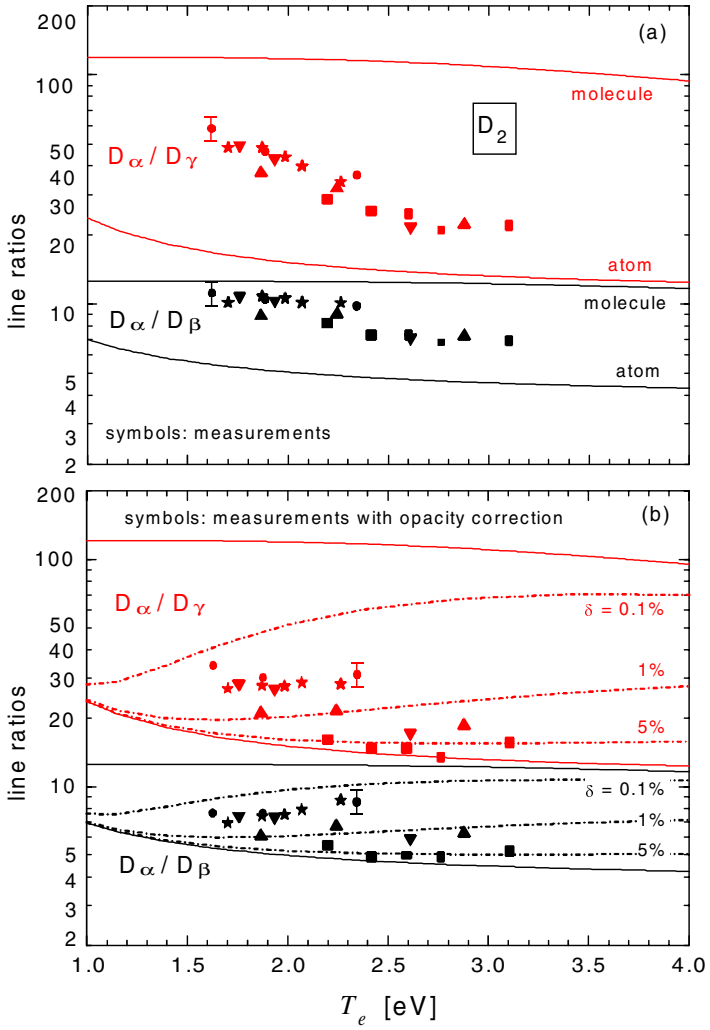

Figure 11. Balmer line ratios of D_2/He mixtures at various pressures with and without correction of the optical thickness for various degrees of dissociation. The symbols denote the mixtures: (square) 10%, (triangle up) 20%, (triangle down) 50%, (circle) 80% and (star) 90% deuterium molecules in helium.

quite important and must be taken into account in the analysis. As an example, figures 10(a) and 11(a) show two measured Balmer line ratios, recorded routinely for a number of hydrogen and deuterium plasmas. Depending on dissociation degree, the H_α/H_β ratio is, for example, expected to be

$$\frac{\dot{N}_{\mathrm{Ph},3,2}}{\dot{N}_{\mathrm{Ph},4,2}} = \frac{n_{\mathrm{H}} X^{a}_{\mathrm{em},3,2}(T_{\mathrm{e}}) + n_{\mathrm{H}_2} X^{\mathrm{M}}_{\mathrm{em},3,2}(T_{\mathrm{e}})}{n_{\mathrm{H}} X^{a}_{\mathrm{em},4,2}(T_{\mathrm{e}}) + n_{\mathrm{H}_2} X^{\mathrm{M}}_{\mathrm{em},4,2}(T_{\mathrm{e}})} \tag{13}$$

with upper and lower limits for pure molecular and pure atomic excitations. The measurements are expected somewhere between these two lines, which are also plotted in figures 10 and 11. The ratios also depend on T_{e}, but to a much lesser extent than the results in equation (11). In the case of hydrogen, some measured values are clearly above the molecular excitation line, indicating a problem, which can again be solved by correcting for the optical thickness of the

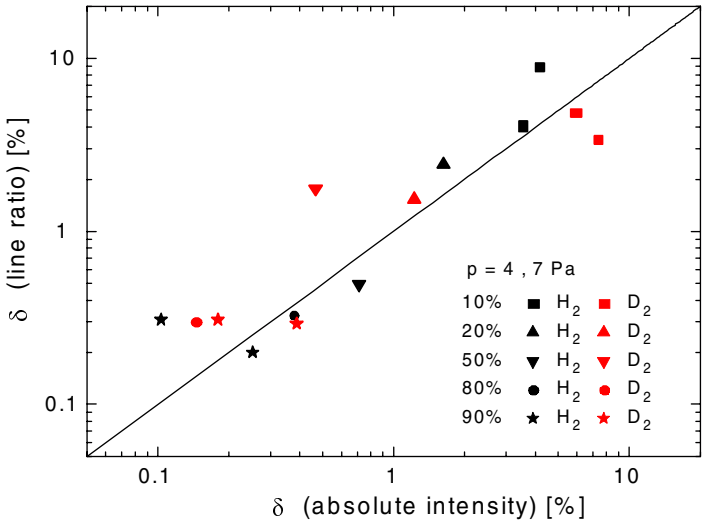

Figure 12. Comparison of results for the dissociation degree from absolute line intensities (average of H_α, H_β and H_γ) and from hydrogen line ratios (average of H_α/H_β and H_α/H_γ).

Lyman resonance lines. Since the highest ratios belong to predominantly dissociative excitation, the results demonstrate that reabsorption is in fact an important process even for the molecular contribution.

In the analysis of the line ratios, the measured radiances, rather than the rate coefficients, were corrected for opacity, i.e. transformed to optically-thin intensities by means of the correction factors k. Then, as given in the lower parts of the two figures, the results are precisely in the expected range and can be interpreted in terms of dissociation degree δ. For that purpose, calculated ratios for $\delta = 0.1\%$, $\delta = 1\%$ and $\delta = 5\%$ are also shown in figures 10 and 11. Both measured line ratios yield quite consistent results for a dissociation degree both in hydrogen and deuterium, as can be concluded from the symbols in these figures. The line ratio method is apparently sensitive in the range between about 0.1 and 5% dissociation degree, but requires very accurate measurements. The estimated uncertainties in relative calibration ($\pm 10\%$) already lead to error bars of a factor of two or more in δ. The H_α/H_γ ratio is superior; however, it becomes very electron density dependent at higher n_e. In deuterium, the ratio of atomic and molecular excitation is more different than in hydrogen, which means that the results from the line ratio method have higher accuracy. The older Johnson and Hinnov rate coefficients for atomic hydrogen [2] lead to clear discrepancies with these experimental results.

A summary and comparison of the two methods for measuring the dissociation degree is shown in figure 12 for the plasma pressures of 4 and 7 Pa. Considering the limited sensitivity of the criteria and the experimental uncertainties, the results are in very good agreement. The measured dissociation degrees are in the same range as typical results from the very sophisticated two-photon LIF method (values for hydrogen RF plasmas: $\delta = 1$–5% [23]). The rate coefficients used for hydrogen and helium excitation, as well as for the dissociative excitation of hydrogen molecules, lead to consistent results within the error limits. When comparing the data, it must be kept in mind that above a few per cent H or D atoms, the ratio method is no longer suitable

and the absolute measurements are superior. On the other hand, at dissociation degrees of the order of 1% or less, two comparable numbers must be subtracted in the latter case, substantially increasing the error bars. Assuming 10% accuracy for the rate coefficients, plus 10% for the system calibration and the spectral line integration for H and He lines, this leads to a factor of two or three in the results shown. The ratio technique is the recommended choice here, even more so for deuterium than for hydrogen, which becomes again quite insensitive below about 0.1%. For 80% or 90% hydrogen in helium, nearly the all the radiation originates from molecular excitation and the degree of dissociation is of the order of 0.1%. In contrast, the degree of dissociation is around 5% in 10% H_2 mixtures in helium and the Balmer radiation is dominated by atomic excitation. In deuterium, the values are always somewhat higher. Dissociative excitation is more important in hydrogen than in deuterium, opacity plays a role in both cases, especially for H_α and D_α. Deviations from a Maxwellian EEDF lead to an over-estimate of the dissociation degree, even more so in the absolute intensity method than the line ratios method.

8. Conclusions

Hydrogen Balmer lines are emitted by plasmas for fusion research or by many plasma reactors for technical applications far from thermodynamic equilibrium. They can be easily recorded and could constitute a convenient diagnostic tool. However, interpretation is not always trivial, even though precise excitation rate coefficients have recently become available. The intensities can be substantially affected by the dissociative excitation of the H_2 and D_2 molecules and by the optical thickness of the Lyman resonance lines. They must be modelled on the basis of collisional-radiative codes including molecular contributions and the appropriate escape factors. Molecular contributions are lower for deuterium than for hydrogen and decrease with the principal quantum number n. In this paper, population escape factors for these plasmas were calculated on the basis of some simplifying assumptions and included in the ADAS program package. Ground-state and dissociative excitation of H_2 and D_2 were computed simultaneously. This results in correction factors for the effective excitation rate coefficients for atoms and molecules and changes in ionization and recombination rates. The consequences of wider emission than absorption profiles were also investigated, but the experiments also require opacity corrections for the molecules. For temperature diagnostics, helium excitation rate coefficients were included.

The described model was applied to the analysis of microwave plasmas in mixtures of hydrogen or deuterium with helium in order to verify the theoretical results. Atom densities and dissociation degrees were derived from two methods, (i) the absolute intensities of three Balmer lines subtracting dissociative excitation, and (ii) the comparison of two Balmer line ratios with those expected for various degrees of dissociation. In both cases, there were clear indications that the opacity had to be included, even for the molecular contribution. After that, consistent results could be obtained within the uncertainties of the measurements and for the cases where the EEDF was not too far from Maxwellian. The dissociation degree in the investigated plasmas varied roughly between 0.1 and 10%, depending on the pressure and the gas mixture, and it was slightly higher in deuterium. Analysis of deuterium plasmas was always somewhat more consistent than hydrogen, due to the lower contribution from dissociative excitation. The results present a basis for the interpretation of Balmer line radiation in various plasmas and demonstrate the pertinent possibilities and difficulties.

References

[1] Hassouni K, Gicquel A, Capitelli M and Loureiro J 1999 *Plasma Sources Sci. Technol.* **8** 494
[2] Johnson L C and Hinnov E 1973 *J. Quantum Spectrosc. Radiat. Transfer* **13** 333
[3] Drawin H W and Emard F 1970 Instantaneous population densities of the excited levels of hydrogen atoms, hydrogen-like ions and helium atoms in optically thin and thick non-LTE plasmas *Report* EUR-CEA-FC-534
[4] Anderson H, Ballance C P, Badnell N R and Summers H P 2000 *J. Phys. B: At. Mol. Opt. Phys.* **33** 1255
[5] Summers H P 1999 *ADAS User Manual Version 2.1* webpage http://patiala.phys.strath.ac.uk/adas, University of Strathclyde, Glasgow
[6] Möhlmann G R, De Heer F J and Los J 1977 *Chem. Phys.* **25** 103
[7] Sawada K and Fujimoto T 1995 *J. Appl. Phys.* **78** 2913
[8] Wenzel U, Behringer K, Carlson A, Gafert J, Napiontek B and Thoma A 1999 *Nucl. Fusion* **39** 873
[9] Irons F E 1979 *J. Quantum Spectrosc. Radiat. Transfer* **22** 1
[10] Tawara H, Itikawa Y, Nishimura H and Yoshino N 1990 *J. Phys. Chem. Ref. Data* **19** 617
[11] Möhlmann G R, Shima K H and De Heer F J 1978 *Chem. Phys.* **28** 331
[12] Fujimoto T 1979 *J. Quantum Spectrosc. Radiat. Transfer* **21** 439
[13] De Heer F J, Hoekstra R, Kingston A E and Summers H P 1992 Excitation of neutral helium by electron impact *Report* JET-P(92)09
[14] Fujimoto T 1995 Private communication
[15] Behringer K 1998 Escape factors for line emission and population calculations *Report* IPP 10/11
[16] Fantz U 1998 *Plasma Phys. Control. Fusion* **40** 1459
[17] Burshtein M L, Komarovskii V A, Penkin N P, Tolmachev Yu A and Federov A N 1989 *Opt. Spectrosc.* **67** 146
[18] Behringer K and Fantz U 1994 *J. Phys. D: Appl. Phys.* **27** 2128
[19] Wouters M J, Khachan J, Falconer I S and James B W 1999 *J. Phys. B: At. Mol. Opt. Phys.* **32** 2869
[20] Celiberto R, Cacciatore M, Capitelli M and Gorse C 1989 *Chem. Phys.* **133** 355
[21] Celiberto R, Cives P, Cacciatore M, Capitelli M and Lamanna U T 1990 *Chem. Phys. Lett.* **169** 69
[22] Schulz-von der Gathen V and Döbele H F 1996 *Plasma Chem. Plasma Proc.* **16** 461
[23] Chérigier L, Czarnetzki U, Luggenholscher D and Schulz-von der Gathen V 1999 *J. Appl. Phys.* **85** 696